Accepted Manuscript

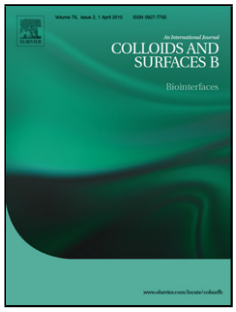

Title: Functional *Micrococcus lysodeikticus* layers deposited by laser technique for the optical sensing of lysozyme

Authors: Valentina Dinca, Diana Zaharie-Butucel, Luciana Stanica, Simona Brajnicov, Valentina Marascu, Anca Bonciu, Andra Cristocea, Laura Gaman, Mihaela Gheorghiu, Simion Astilean, Alina Vasilescu

PII: S0927-7765(17)30799-3
DOI: https://doi.org/10.1016/j.colsurfb.2017.11.058
Reference: COLSUB 9009

To appear in: *Colloids and Surfaces B: Biointerfaces*

Received date: 11-9-2017
Revised date: 13-11-2017
Accepted date: 22-11-2017

Please cite this article as: Valentina Dinca, Diana Zaharie-Butucel, Luciana Stanica, Simona Brajnicov, Valentina Marascu, Anca Bonciu, Andra Cristocea, Laura Gaman, Mihaela Gheorghiu, Simion Astilean, Alina Vasilescu, Functional Micrococcus lysodeikticus layers deposited by laser technique for the optical sensing of lysozyme, Colloids and Surfaces B: Biointerfaces https://doi.org/10.1016/j.colsurfb.2017.11.058

Functional *Micrococcus lysodeikticus* layers deposited by laser technique for the optical sensing of lysozyme

Valentina Dinca[1], Diana Zaharie-Butucel[2], Luciana Stanica[3,] Simona Brajnicov,[1,4], Valentina Marascu,[1,5], Anca Bonciu[1,5], Andra Cristocea[6], Laura Gaman[7], Mihaela Gheorghiu[3], Simion Astilean[2], Alina Vasilescu[3]*

[1]*National Institute for Laser, Plasma and Radiation Physics (INFLPR, 409 Atomistilor, PO Box MG-36, 077125, Magurele, Bucharest, Romania,*

[2]*Nanobiophotonics Center, Interdisciplinary Research Institute in Bio-Nano-Sciences, Treboniu Laurian 42, Cluj-Napoca, Romania,*

[3]*International Centre of Biodynamics, 1B Intrarea Portocalelor, 060101, Bucharest, Romania,*

[4]*University of Craiova, Faculty of Mathematics and Natural Science, 13 Alexandru Ioan Cuza, 200585 Craiova, Romania,*

[5]*University of Bucharest, Faculty of Physics, 405 Atomistilor, 077125 Bucharest-Magurele, Romania,*

[6] *Fundeni Clinical Institute, Department of Gastroenterology and Hepatology, Bucharest, Sos. Fundeni nr. 258, Romania,*

[7]*"Carol Davila"University of Medicine and Pharmacy, Faculty of Medicine, Department of Biochemistry, 8 B-dul Eroilor Sanitari 76241, Bucharest, Romania.*

*corresponding author: Alina Vasilescu, e-mail: avasilescu@biodyn.ro, tel:+40 310 4354

STATISTICAL SUMMARY: 5836 words, 7 figures, 1 table

Graphical abstract

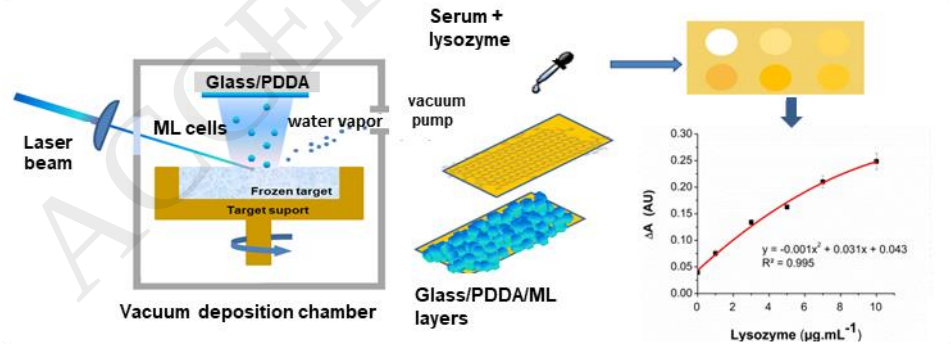

Highlights:

- functional layers of *Micrococcus lysodeikticus* deposited via MAPLE on glass slides

- bacterial interfaces sensitive to lysis by lysozyme were used as optical biosensors
- MAPLE-deposited biointerfaces were compared to ones deposited via layer-by-layer
- lysozyme detected in undiluted serum in the clinical range up to 10 μg mL^{-1}

Abstract

Whole cell optical biosensors, made by immobilizing whole algal, bacterial or mammalian cells on various supports have found applications in several fields, from ecology and ecotoxicity testing to biopharmaceutical production or medical diagnostics. We hereby report the deposition of functional bacterial layers of *Micrococcus lysodeikticus (ML)* via Matrix-Assisted Pulsed Laser Evaporation (MAPLE) on poly(diallyldimethylamonium) (PDDA)-coated-glass slides and their application as an optical biosensor for the detection of lysozyme in serum. Lysozyme is an enzyme upregulated in inflammatory diseases and *ML* is an enzymatic substrate for this enzyme. The MAPLE-deposited bacterial interfaces were characterised by Scanning Electron Microscopy (SEM), Atomic Force Microscopy (AFM), Fourier-Transformed Infrared Spectroscopy (FTIR), Raman and optical microscopy and were compared with control interfaces deposited via layer-by-layer on the same substrate. After MAPLE deposition and coating with graphene oxide (GO), *ML*-modified interfaces retained their functionality and sensitivity to lysozyme's lytic action. The optical biosensor detected lysozyme in undiluted serum in the clinically relevant range up to 10 μg mL^{-1}, in a fast and simple manner.

Keywords: MAPLE, *Micrococcus lysodeikticus*, whole cells, optical biosensor, lysozyme

1. Introduction

Whole cell biosensors, made by immobilizing whole algal, bacterial or mammalian cells on various supports, with detection by optical [1, 2] or electrochemical methods [3-5] have found applications in several fields, from environmental monitoring to biopharmaceutical production [6] or medical diagnostics [7].Various procedures like spin coating, drop casting, dip coating, entrapment in polymers during electropolymerization [8], electrophoretic deposition [9] have been described [10] for surface functionalization with whole cells via adsorption, electrostatic interactions [11], covalent immobilization [12], affinity binding [13] or physical entrapment [14].

Relatively new in the biointerfaces and biosensing fields, especially for transferring cells, the laser deposition method shows great promise for obtaining controlled layers of natural or

synthetic compounds with improved performances, without the issues related to sample uniformity, contamination, and solvent use, usually associated with typical surface functionalization techniques such as drop casting, dip coating or spin coating. MAPLE technique was developed for transferring organic and inorganic materials onto solid substrates, proving to be a flexible method for transferring functional sensitive organic compounds in a controlled manner [15]. There are various applications in the field of medicine, biology, bio- and chemical sensing where MAPLE proved its versatility in transferring natural and synthetic polymers [16, 17], nanoparticles [18] or to embed various drugs and proteins within a polymeric matrix [19]. Although laser induced forward transfer was used for transferring liposomes and mammalian cells [20, 21], no work has been reported on the use of MAPLE for transferring cells while maintaining cellular activity. Responding to this challenge, in this work, we present the development of *ML* whole cell layers, deposited by MAPLE on PDDA-coated glass slides. To investigate the preservation of cell functionality, the interfaces were coated with GO and tested for the determination of lysozyme in serum. Lysozyme is a 14.3 kDa enzyme whose concentration in human serum is a non-specific biomarker for inflammatory diseases, as is upregulated in several diseases including AIDS, pulmonary tuberculosis, sarcoidosis or Inflammatory Bowel Disease (IBD) [22]. Moreover, lysozyme catalyses the lysis of β-1,4 glycosydic linkages between N-acetylmuramic acid and N-acetylglucosamine residues in the peptidoglycan of bacterial cell walls [23]. *ML* is a typical substrate for this enzyme, used to determine the enzymatic activity of lysozyme via turbidimetry [24].

We have recently shown that Au interfaces modified via the layer-by-layer (LBL) method with (PDDA), GO and *ML* conveniently allow the detection of lysozyme in serum by Surface Plasmon Resonance (SPR) [25]. Among the more established immobilization methods, LBL deposition, consisting in the alternating deposition of polyanionic and polycationic layers (of opposing charge) [26], was demonstrated to be a gentle, yet effective method for immobilizing enzymes and cofactors which retain their functionality [27] as well as a convenient way to modify various types of interfaces for promoting or preventing cell attachment [11]. In our previous work, when the ML bacteria were adsorbed on an Au interface, incubation with lysozyme resulted in their lysis and desorption from the interface with corresponding decrease in the SPR signal [25]. GO was deemed critical for the stability of the interfaces in serum, emphasizing the importance of the sensing interfaces architecture.

Starting from these principles, we investigate here the applicability of MAPLE deposition to develop controlled interfaces for optical detection of lysozyme as alternatives to SPR devices. The studies with MAPLE-deposited devices were complemented by similar tests with PDDA/ML/GO slides prepared using LBL approach, optimised and used as reference interfaces for detection of lysozyme in serum.

2. Materials and methods

2.1. Materials

Fetal bovine serum (FBS) and bovine serum albumin (BSA) were purchased from Gibco, Thermo Fisher Scientific, USA. Human lysozyme, GO, *Micrococcus lysodeikticus*, PDDA and all other reagents were purchased from Sigma-Aldrich, Germany. Microscope slides with dimensions of 76x26 mm were provided by Roth, Germany. Two human serum samples from patients suffering of IBD were kindly provided by Dr. Ionescu Andra (Fundeni Clinical Institute, Department of Gastroenterology and Hepatology, Bucharest, Romania) in accordance with the local ethical committee and the ethical obligations of the Declaration of Helsinki. The participants underwent peripheral blood sampling into heparin-containing tubes (5 ml) after an overnight fast. After centrifugation, 548 g for 15 min at 4°C, the resulting plasma was placed on ice prior to storage at -80°C until further analysis.

2.2. Preparation of PDDA-coated glass substrates

Microscope slides were cleaned in diluted soap and hot water, followed by rinsing with water and ethanol and by a 15 min exposure to UV-ozone. A volume of 1 mL of 5% PDDA solution in 0.1 M NaCl was placed on the surface of a clean slide and was left to adsorb for 1h. The slide was rinsed with water and then dried under N_2 stream.

2.3. Preparation of PDDA/ML/GO functional interfaces via layer-by-layer

PDDA-coated slides were exposed to 1 mL of 0.25 mg mL^{-1} suspension of ML in water and left to adsorb for 20 min -1 h. After rinsing with water and drying under N_2 stream, the slides were covered with 1 mL of 0.5 mg mL^{-1} GO solution and left at room temperature for 1 h. Finally, after another rinsing and drying step, the functionalised PDDA/ML/GO interfaces were kept in the fridge until used.

2.4. Preparation of PDDA/ML/GO functional interfaces by MAPLE deposition

The solid targets for MAPLE deposition have been prepared by freezing, under continuous stirring, in liquid nitrogen, a solution of *Micrococcus* bacteria (1 % w/v in water). The solid/frozen target obtained was placed in the vacuum chamber of the MAPLE set-up and irradiated with a SURELITE II (Amplitude Laser Group, Continuum, USA) Nd:YAG laser (5-7 ns pulse duration) at 266 nm and 10 Hz repetition rate. The laser fluence used was set between 0.6 and 1.2 J cm^2 and the number of pulses used was 48000. The energy of the pulsed laser beam reaching the target is converted into thermal energy by photochemical processes and evaporation takes place, leading to bacteria transport and deposition on the substrates (PDDA-coated glass or Si), placed at 3 cm and parallel to

the target. In order to avoid the damage caused by multiple pulses onto the same place which would lead to cells destruction, the target was rotated with 20 rpm.

2.5. Structural characterization of *Micrococcus lysodeikticus*-functionalized interfaces

FTIR was applied to study the characteristic vibrations of functional groups in the ML bacteria deposited on silicon wafer by MAPLE and LBL. The FTIR measurements were carried out with a Jasco FT/IR-6300 type A spectrometer in the 400-7800 cm^{-1} range, with a resolution of 4 cm^{-1}. The spectra were measured in absorption mode, by accumulation of 1024 scans, and using a Rosenfeld apodization function.

2.6. Morphological characterization of *Micrococcus lysodeikticus*-functionalized interfaces

The obtained features were investigated by AFM and SEM. The AFM measurements were carried out in non-contact mode, using silicon probes (PPP-NCHR, Nanosensors) with 42 N/m force constant, 330 kHz resonance frequency and less than 7 nm radius (nominal values). Topography images were recorded on 40 μm × 40 μm areas. For SEM, a JSM-531 microscope (FEI Inspect S) operating at 5 kV was used to analyze the deposited samples in more detail.

2.7. Raman analysis

Raman measurements were performed using a confocal Raman microscope (CRM alpha 300R from WITec GmbH, Germany), using a 532 nm Nd-Yag laser excitation line entering the microscope through a mono-modal optical fibre and directed through a 100× dry microscope objective towards the samples fixed on an anti-vibration stage. The Raman backscattered light, collected through the objective, was passed through a multimode optical fiber (100 μm diameter) and focused into a spectrometer equipped with a 1024 × 128 pixel CCD camera operating at - 60 °C (DV401-BV, Andor). The point spectra were acquired with 10 s integration time. The Raman mapping was performed with 0.5 s integration time, over a 10 × 10 μm^2 area, divided into 40 × 40 points/line. The spectra deconvolution was made with a combination of Lorentz and Breit–Wigner–Fano (BFW) lines suitable for carbon structures [28]. WITec Project Plus software () was utilized for spectral and image processing and analysis.

2.8. Optical microscopy

Optical microscopy phase contrast images were acquired with a Nikon Eclipse TS 100 microscope (Nikon, Japan), and a 20 × 0.4 objective. The images were further on processed using ImageJ software (NIH, USA).

2.9. Determination of lysozyme concentration in serum based on its lytic activity

The determination of lysozyme in the fetal bovine serum sample used for spiking experiments was based on its enzymatic activity using a classic turbidimetric assay [24] and calculations were based on the calibration curve with human lysozyme.

2.10. Sensing of lysozyme in serum with ML-functionalised interfaces

ML-functionalised surfaces deposited by MAPLE or LBL were "blocked" with GO (0.5 mg mL^{-1} solution in water) for 30 min, after which were rinsed with water and dried under nitrogen stream. A 15 µL drop of lysozyme-containing solution (calibration standard or sample) was spotted on the ML interface and left for 10 min, after which the interface was rinsed with water and dried. The absorbance spectrum of the sample spot in the range 350-700 nm before and after the test with lysozyme was collected with a Thermo Evolution Pro spectrophotometer. For quantitative determinations, the decrease in the absorbance of the sample spot at 700 nm was correlated with the concentration of lysozyme in the sample. In an alternative approach, the ML interfaces exposed to lysozyme were scanned against a black background with an office scanner and the images were analysed using ImageJ software (NIH, USA). The decrease in the intensity of the sample spots compared to the background intensity of the slide (unreacted with lysozyme) was divided by the analysed area and was correlated with the concentration of lysozyme.

3. Results and discussions

3.1 "Reference" *ML*-coated interfaces deposited via LBL

ML- functionalized glass slides were prepared via LBL to be used as "reference" sensing interfaces for the optical detection of lysozyme in serum. The LBL deposition was optimized starting from previous work with plasmonic interfaces [25]. Glass slides were first coated with PDDA then left in contact with suspensions of ML of different concentrations. Optimization studies have been performed with 0.1 to 2 mg mL^{-1} ML suspensions in water, left to adsorb for 20 - 120 min. Measurements of ML-functionalized slides by UV-VIS spectrometry have shown that the best results, i.e most opaque and uniform bacterial coatings were obtained with 1 mg mL^{-1} ML left to adsorb for 20 min (Electronic Supplementary Material, Fig S1).

Deposition of additional, successive layers of PDDA/ML did not bring any improvements. The uniformity and reproducibility of bacterial films were evaluated by measuring the absorbance of glass slides in the VIS range. The RSD of the absorbance at 700 nm measured in different spots on the slide was between 0.77 and 3.45% (n=5 spots/slide), proving that a uniform bacterial layer was deposited by LBL. The average absorbance at 700 nm was 0.386±0.011 for n=4 different slides from the same fabrication batch, indicating a good reproducibility. The optimized *ML*-coated slides were used as reference interfaces when evaluating the slides with bacteria deposited by MAPLE.

3.2 Functional interfaces with ML deposited by MAPLE

ML films deposited on PDDA-coated slides by MAPLE (schematically represented in Fig. 1) were evaluated to check MAPLE compatibility with obtaining functional bacterial coatings.

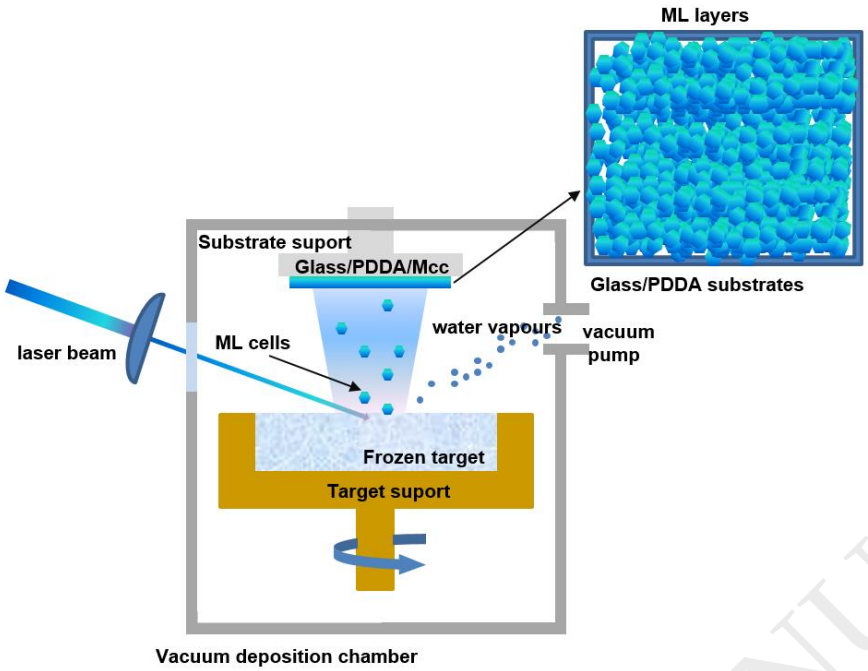

Fig. 1 Schematic representation of the deposition process of ML films by MAPLE onto PDDA functionalized glass substrates

To determine the optimal parameters for MAPLE deposition, morphological changes of the bacterial film deposited by MAPLE were compared with the characteristics of the coatings obtained by LBL (considered as reference) using AFM and SEM. Moreover, the spectral band assignments from representative infrared spectrum in the 400-4000 cm^{-1} region of the MAPLE and reference LBL samples were analyzed and compared. As shown in Fig. 2, the deposition of whole bacterial cells was possible only for specific parameters.

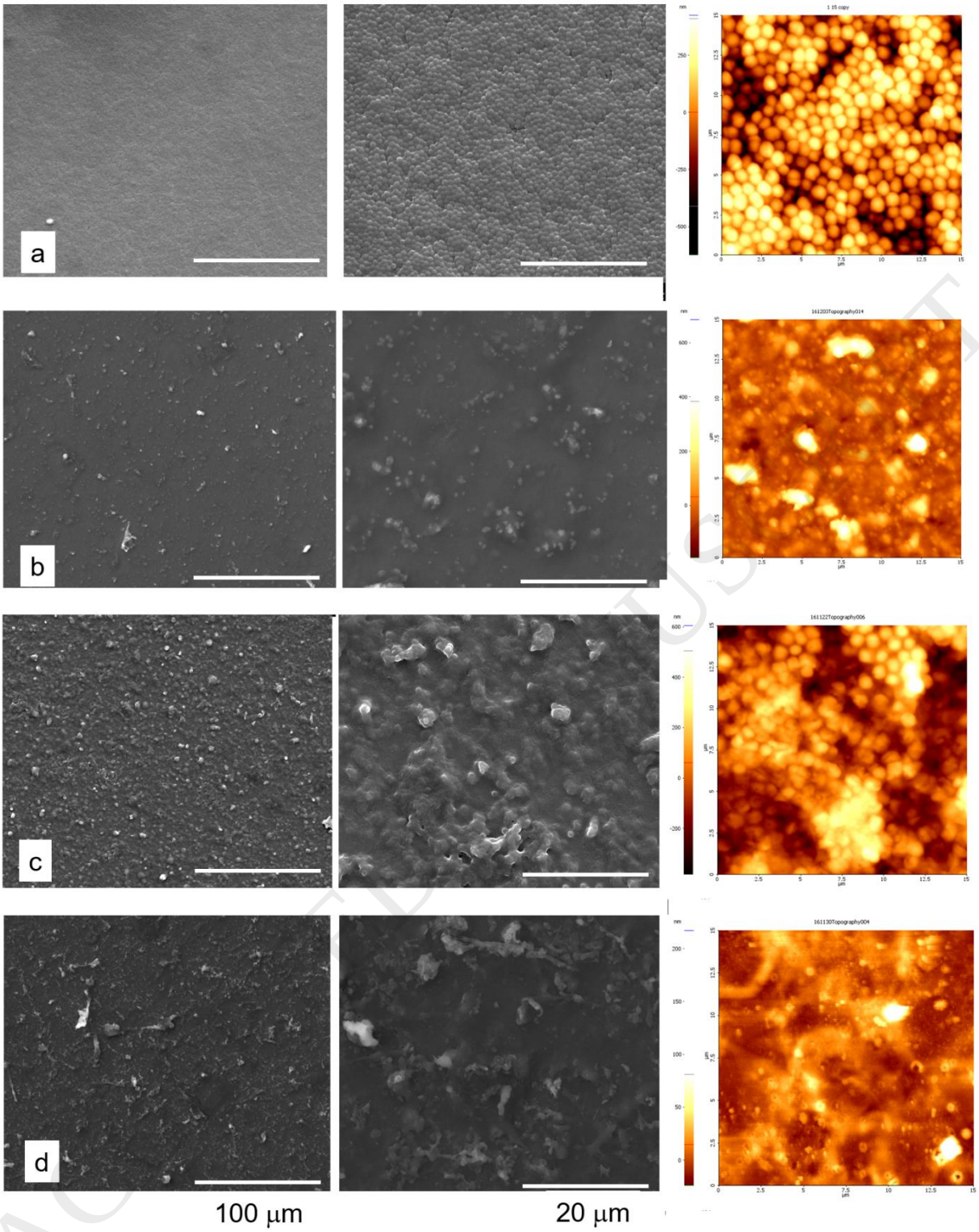

Fig. 2 SEM and the corresponding AFM (15 µm x 15 µm) images of ML bacteria deposited on PDDA substrates by LBL (a) and MAPLE at 0.6 J cm-^{2} (b), 0.8 J cm-^{2} (c), 1.2 J cm-^{2} (d)

In control samples (LBL), the cells formed a uniform layer of bacteria, according to SEM and AFM images (Fig. 2a). Noteworthy, in the case of MAPLE samples, the AFM imaging revealed the presence of whole bacteria deposited onto glass/PDDA surfaces, but with different

configuration or arrangement on the surface depending on the used laser fluence. Based on morphological analysis of the deposited bacteria, as well as on FTIR spectra shown in Fig. 3, an optimal deposition of ML bacteria was obtained only for 0.8 J cm^{-2}. A lower value, 0.6 J cm^{-2} generally used as the maximum fluence for attaining successful deposition of smaller molecule compounds (polymers or proteins) led to transfer of ML bacteria with lower density on the surface. Higher fluence, above 0.8 J cm^{-2} led to an increase of bacteria debris on the surface further confirmed by FTIR measurements in Fig 3, revealing modifications that could be assigned to bacteria walls breaking. If the island-like cell clusters on the surface were characteristic for fluences up to 0.8 J cm^{-2}, higher values of 1.2 J cm^{-2} led to cell membrane destruction and deposition of clusters of deflated and damaged bacteria. Whereas the control ML surfaces are characterized by 160 nm roughness and 1.8 μm thickness, the ML surfaces deposited by MAPLE were characterized by lower roughness, from 142 nm ML layers (thickness 1.25 +/- 0.2 μm) obtained at 0.8 J cm^{-2}, to 82 nm layers (thickness 0.8 +/- 0.1 μm) for 0.6 J cm^{-2} and to 18 nm (and thickness below 500 nm) in the case of ML coatings obtained with fluences of 1.2 J/cm^{-2}. The decrease of thickness and roughness of the layers obtained with higher fluences than optimum can be explained by the cell breaking and deposition of cell membrane as coating instead of whole cell. At the optimal laser fluence of 0.8 J cm^{-2}, MAPLE deposition had no significant influence on the rigidity of the cells when compared with those obtained via LBL.

3.3 FTIR analysis

FTIR measurements were performed to analyze the differences induced by deposition methods (MAPLE and LBL) in the functional groups within the ML samples. As seen in Fig. 3, the spectrum of MAPLE-deposited *Micrococcu*s showed absorptions similitudes with that of the LBL–deposited sample only for specific MAPLE parameters. Moreover, for high fluences, there are several supplementary bands. For example, the absorption band at 1744 cm^{-1} assigned to the ester νC=O stretching vibration for *Micrococcus* obtained by MAPLE, was previously found in literature for other type of ML bacteria as a result of the high proportion of unsaturated acyl chains in triglycerides [29], however, for the LBL one, no such band was noticed.

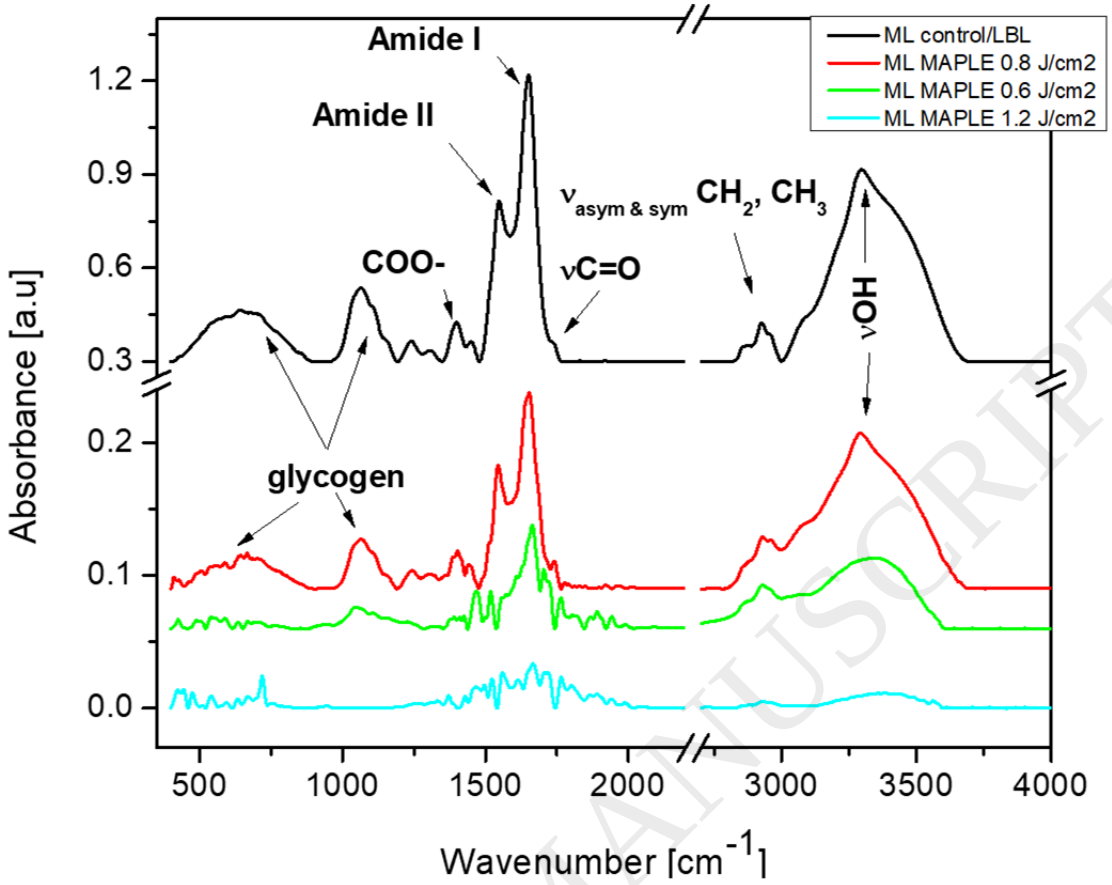

Fig. 3 FTIR spectra of ML bacteria deposited on Si substrates by drop casting (black line-ML control) and MAPLE at 0.6 J cm^2(green line), 0.8 J cm^2(red line), 1.2 J cm^2 (blue line)

The location of amide I absorption is generally sensitive to protein conformation, any differences implying conformational changes in cell proteins [30]. As can be seen from Fig. 3, when laser fluence increased above 0.8 J cm^{-2}, major modifications appear, especially envisaging the amide I and II and other typical functional peaks such as those corresponding to glycogen. One can note that amide I was preserved for both MAPLE and LBL sample (1641 cm^{-1}) when laser fluences were below or equal to 0.8 J cm^{-2}. Amide II band was observed at 1520 cm^{-1} but modification was already observed for all fluence values except 0.8 J cm^{-2}. The band at 1391 cm^{-1} is due to COO$^-$ symmetric stretching vibration of amino acid side chains and fatty acids [31]. Other peak specific to *Micrococcus* was observed around 1342 cm^{-1} attributed to the stretching mode of carboxylic acids [31]. As can be seen in Fig. 3, in the region of 2800 – 4000 cm^{-1}, the absorptions from ML deposited via LBL are present also in the ML sample deposited via MAPLE. The absorption band from 3337 cm^{-1} shows the presence of the stretching mode of νOH, while the stretching mode of

asymmetrical νCH_3 and νCH_2 vibrations bands from 2932 cm^{-1} appears due to lipids [31, 32]. Based on the observations related to coatings morphology and FTIR analysis, the chosen fluence for our experiments was 0.8 J cm^{-2}.

3.4 GO-coated ML interfaces

Before testing with serum, the PDDA/ML interfaces, either obtained by MAPLE or LBL were additionally coated with GO. This step was found necessary to avoid desorption of bacteria in serum in the absence of lysozyme, similar to our previous observations by SPR [25]. The GO-coated interfaces were characterised by Raman spectroscopy and optical microscopy experiments (Fig. 4).

As presented in Fig. 4A, the Raman spectra of PDDA/ML emphasize a ML band at 2900 cm^{-1} attributed to non-specific organic $>CH_2$ and $-CH_3$ stretching vibrations typical for bacteria [33]. Generally, the fingerprint region 1200–1800 cm^{-1} is used to clearly identify the specific bacteria, but to validate the presence of ML bacteria, we simply monitor the high energy band. Parallel optical microscopy images show the presence of numerous bacteria on the slide, with a relatively uniform distribution. The appearance of ML coated slides is preserved coating with GO (Fig. 4A); however, the Raman spectrum of PDDA/ML/GO slides is dominated by the features of GO, respectively the D and G bands around 1350 and 1590 cm^{-1}.

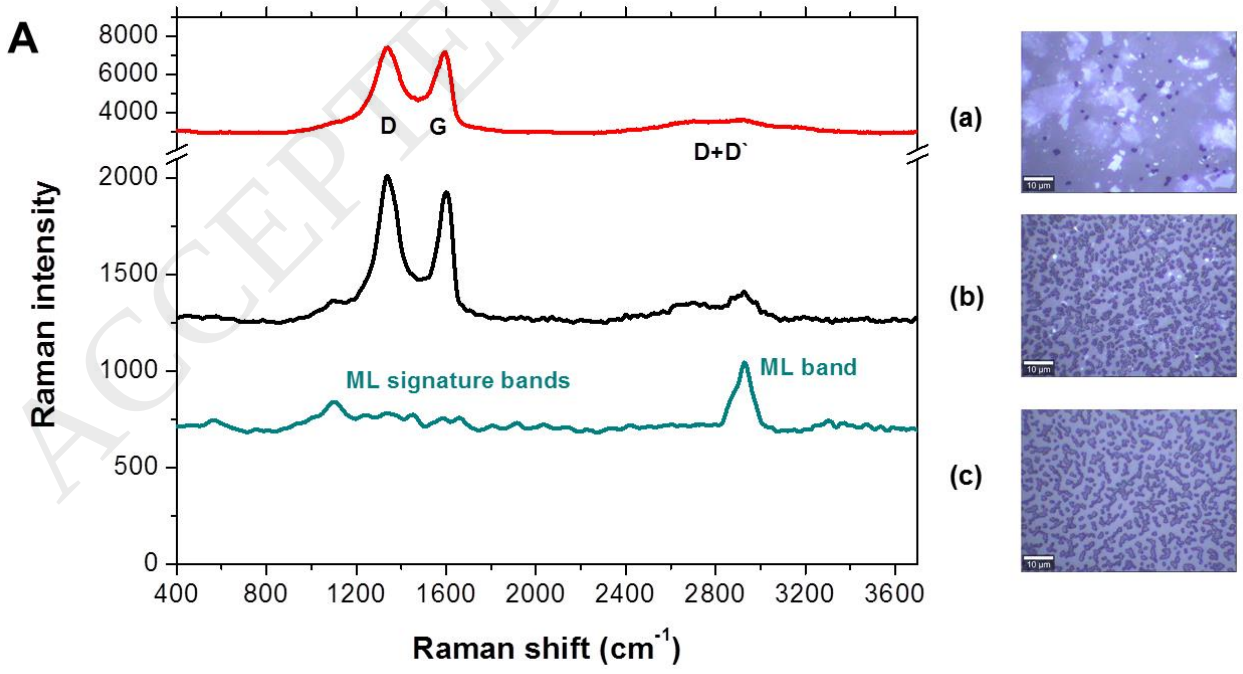

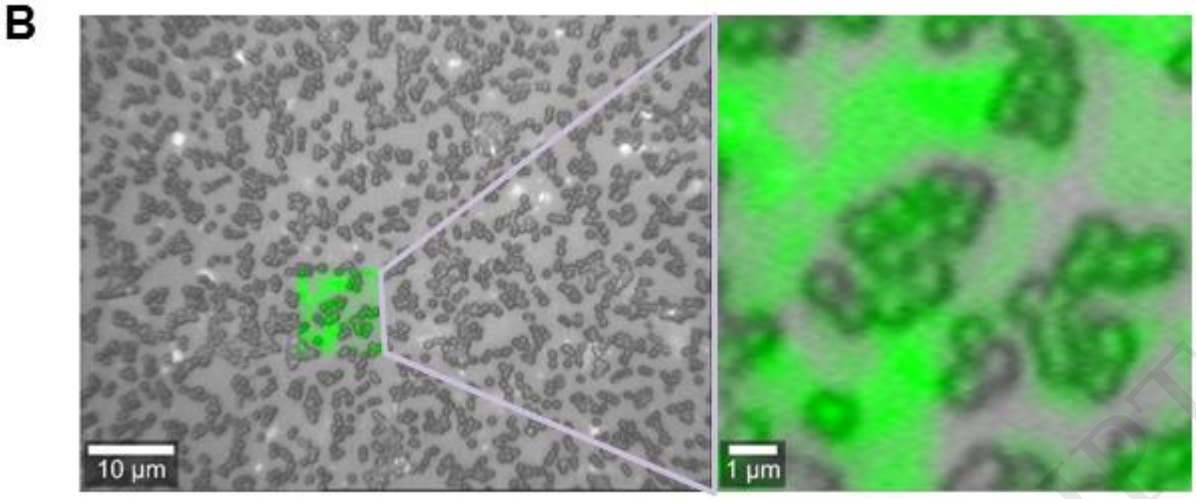

Fig. 4 (A) Raman analysis and corresponding optical microscopy images of interfaces deposited by LBL and coated with GO: (a) PDDA/GO/ML, (b) PDDA/ML/GO, (c) PDDA/ML. (B) Raman maps obtained by representing the intensity of the G band in GO, superposed on the optical microscopy images of ML-interfaces deposited by LBL and coated with GO

For the PDDA/GO/ML sample the GO sheets are readily visible in the optical images and so are the specific D, G and D+D bands in the Raman spectrum. Visually, the slides appear transparent, as no or very little ML bacteria are adsorbed. Numerous bacteria are observed on PDDA/ML/GO sheets yet the Raman spectrum is dominated by the signals from GO. In PDDA/ML the bacteria are numerous and their signal is also seen in Raman spectrum thanks to the absence of GO. These experiments show that ML is not adsorbed on GO but is strongly adsorbed on PDDA. GO is strongly adsorbed on PDDA even when the surface is well covered by ML bacteria. Deposition of ML bacteria via an LBL approach consisting in first adsorbing a positively charged PDDA layer on glass, to which negatively charged ML or GO can attach is thus justified.

Coating PDDA/ML interfaces with an additional layer of GO was found necessary to avoid desorption in serum. Raman maps of the G band intensity in GO, superposed on the optical microscopy images, unambiguously show that GO is adsorbed on PDDA and to a limited extent on ML bacteria, explaining the increased stability of the bacterial layer to desorption by serum (Fig. 4B).

3.5 Application of *ML*-functionalised interfaces for lysozyme sensing in serum

3.5.1 Analytical performaces of biosensors based on MAPLE and LBL –deposited bacteria

To check whether the *ML* bacteria retain their functional integrity after deposition by MAPLE and to prove the advantages of MAPLE deposited bacterial interfaces in sensing, we have evaluated their susceptibility towards lysis by lysozyme. We have compared the MAPLE deposited interfaces

with similar ones obtained by the LBL method. Thus, the PDDA/ML/GO biosensor interfaces were investigated for their utility for lysozyme detection, by applying a volume of 15 µL of FBS spiked with different amounts of human lysozyme (0-10 µg mL^{-1}) on a spot on sensor surface. After 10 min, the interfaces were rinsed with water and dried.

The films of ML bacteria deposited on PDDA-covered slides were found to be stable in undiluted serum in the absence of lysozyme. Furthermore, the ML bacteria preserve their sensitivity to lysozyme, as shown by optical microscopy images (Fig. 5 A and B). After interaction with lysozyme-containing serum, the bacterial coverage decreases on the interfaces deposited by MAPLE, similarly to changes on the control LBL interfaces (Fig. 5 C and D).

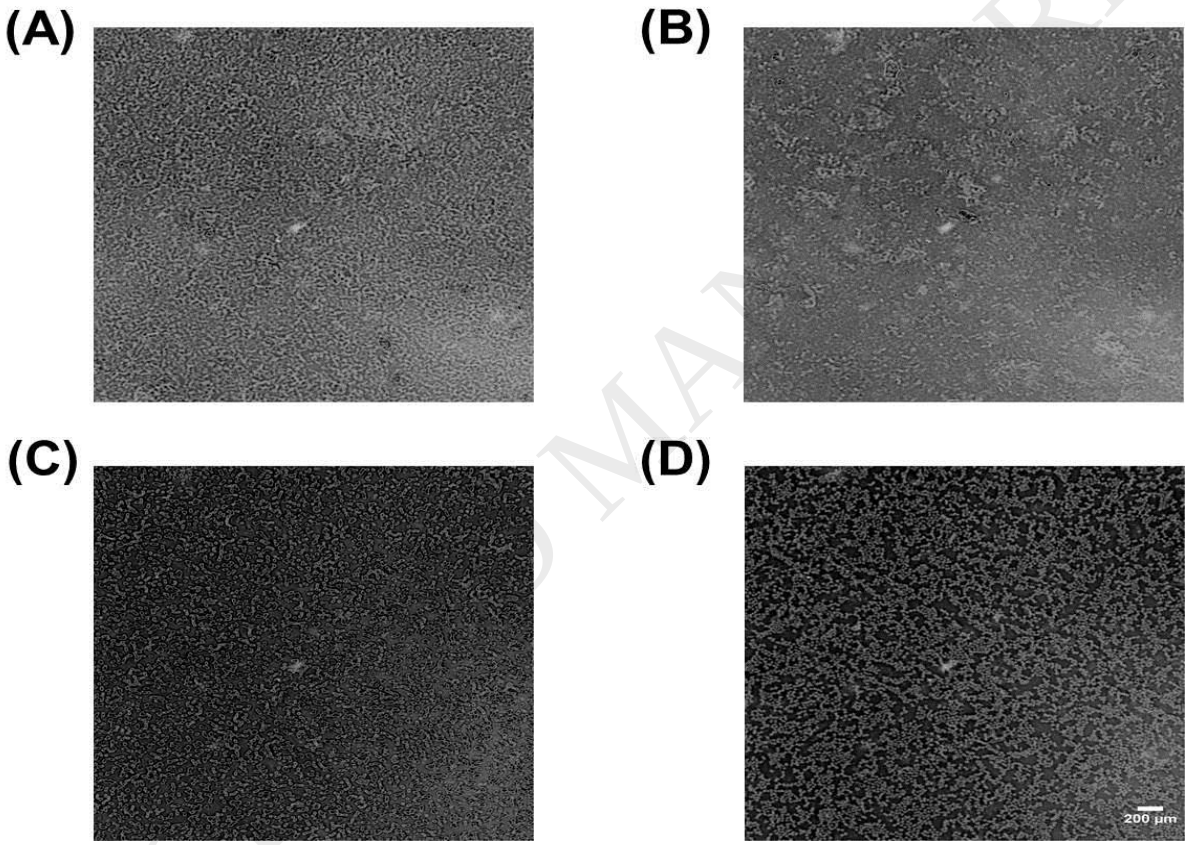

Fig. 5 Optical microscopy phase-contrast images of MAPLE-deposited interfaces before (A) and after the test (B) with serum containing lysozyme, respectively LBL-deposited interfaces before (C) and after (D) the test with serum containing lysozyme. Images were inverted for better clarity, (scale 200 µm)

Correlated with the phase-contrast images, the changes in the intensity of the sample spot after the exposure to serum was evaluated by two alternative methods: (1) by UV-VIS spectrophotometry, measuring the absorbance of the ML-functionalised slides in the range 350-700 nm and (2) by

scanning the slide and analysing the optical image by ImageJ. The incubation time of the biosensors with serum samples was investigated in the range from 5 to 20 min, with optimum at 10 min interaction (not shown; duration further used in all tests).

The absorbance spectra of ML films significantly change following incubation with serum spiked with lysozyme (Fig. 6). Lysozyme lyses the bacteria and induces desorption from the PDDA interface in a concentration-dependent manner. In particular, the absorbance at 700 nm is a reliable analytical parameter, allowing to build calibration curves showing a linear range of 1-10 µg mL^{-1} (Fig. 6) with a calculated detection limit of 0.5 µg mL^{-1}. These data confirm the feasibility of using ML-functionalised interfaces to quantitatively detect lysozyme in serum.

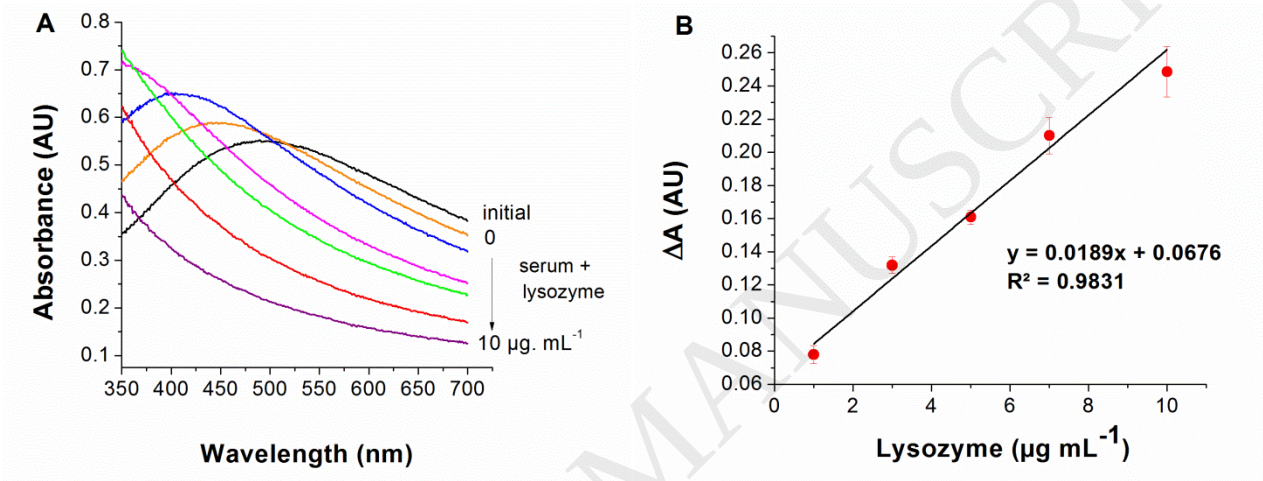

Fig. 6 (A) Absorbance spectra in the range 350-700 nm of PDDA/ML/GO slides following incubation with bovine serum spiked with different concentrations of lysozyme from 0 to 1, 3, 5, 7 and 10 µg mL^{-1}, respectively. (B) Corresponding calibration curve for lysozyme obtained by taking as analytical parameter the variation in absorbance at 700 nm following incubation with spiked serum

Visually, application of lysozyme-spiked serum determines a change in the slide appearance from mate yellowish to clear, due to desorption of bacteria, confirming the previous absorbance measurements and microscopy images. The decrease in the intensity of the sample spots correlates with lysozyme concentration in the samples (Fig. 7 A and B). Compared to UV-VIS spectrometry and optical microscopy, taking a picture of the slide and measuring the sample spot intensity with image analysis software is a simple, cheaper alternative not requiring expensive instrumentation. The analytical range of ML interfaces demonstrated here corresponds to clinically relevant concentrations. Thus, while normal lysozyme levels in serum are in the range 0.46-2.96 µg mL^{-1}, in patients suffering from IBD the concentrations of lysozyme can be in excess of 5 µg mL^{-1} [34].

.

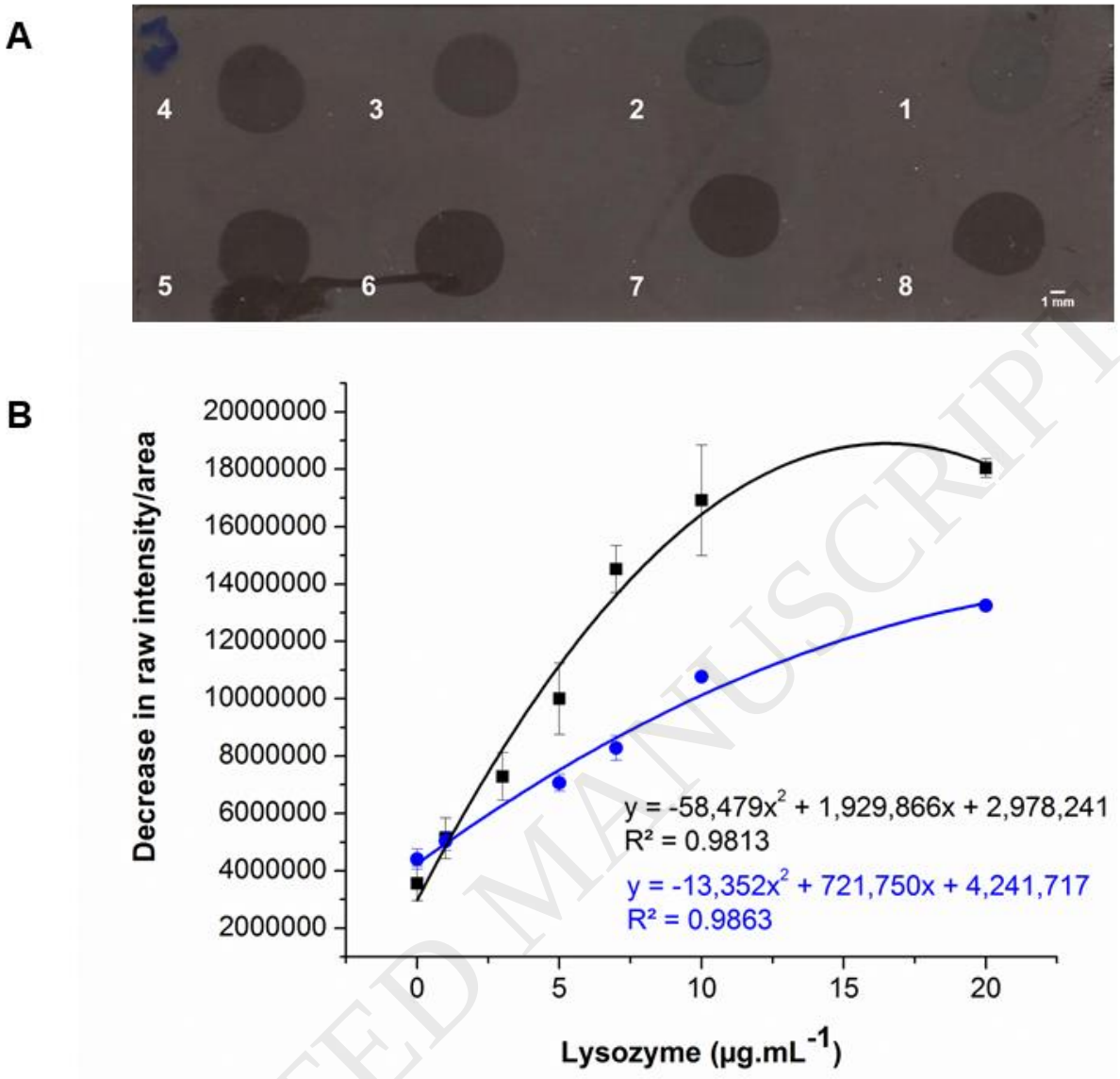

Fig. 7 (A) Photograph of a PDDA/ML/GO 76x26 mm slide showing desorption of ML bacteria from the spots exposed to lysozyme-containing FBS: from spots 1 to 8, serum samples spiked with 1; 3; 5; 7; 10; 20; 50 and 100 µg mL^{-1}, respectively. (B) Calibration curve with LBL (black, squares) and MAPLE-deposited ML interfaces (blue circles)

While both LBL and MAPLE-deposited ML interfaces are susceptible to lysozyme's action, the calibration curves show a slightly higher sensitivity of LBL interfaces. The results of this initial study on MAPLE deposition of ML bacteria emphasize that MAPLE is adequate for depositing bacterial layers without critically affecting the integrity of cell walls and the functionality of bacteria. Compared to LBL, where the steps in slide functionalization were manually performed, MAPLE offers a good control of deposition. More sensitive biosensors for lysozyme have been

reported in literature (Electronic Supplementary Material Table S1): for example, detection limits in the femtomolar range have been achieved with aptamer-based biosensors and either Surface Enhanced Raman Spectroscopy (SERS)[35] or electrochemical detectors including various nanomaterials such as vertically aligned nitrogen doped carbon nanotubes[36], reduced graphene oxide[37] or multiwalled carbon nanotubes and gold nanoparticles[38]. However, due to their sensitivity these biosensors required large sample dilution factors and some also involved expensive instrumentation[35] or rather complex design[38]. By comparison, our sensor is quite simple and allows direct analysis of undiluted serum. Upon further optimization of additional MAPLE parameters besides laser fluence (e.g. target characteristics, distance and repetition rate), the optical test described here, enabled by MAPLE-deposited ML layers can be implemented as a fast test for lysozyme in serum.

3.5.2 Analysis of human serum samples

Two human serum samples and two FBS samples were analysed with the ML-functionalised slides obtained by MAPLE and LBL. As shown in Table 1, there is a good agreement between the results obtained with the ML interfaces deposited by MAPLE and the reference ones deposited by LBL.

Table 1 Analysis of serum samples with ML-functionalised interfaces

Sample	Lysozyme (μg mL^{-1})	
	PDDA/ML slides deposited by MAPLE	PDDA/ML slides deposited via LBL
Human serum 1	5.14±0.06	5.13±0.87
Human serum 2	6.10±0.24	6.72±0.91
Bovine serum	not detected	not detected
Bovine serum spiked with 7 μg/mL lysozyme	6.75±0.35 Recovery: 96.46±5.00 %	7.23±2.14 Recovery:103.26 ±30.61%

Moreover, the recovery values calculated by considering the amount of lysozyme detected with the ML slides versus the theoretical amount spiked in bovine serum indicate a good accuracy of lysozyme detection with both ML interfaces.

4. Conclusions

The deposition of functional ML bacteria on PDDA-coated glass slides by MAPLE was successfully demonstrated. The PDDA layer ensured an adhesive, positively charged layer onto which ML bacteria could be deposited and retained due to opposite charges. SEM, AFM topography images of the bacteria films together with FTIR measurements were used as confirmation that ML was successfully deposited as whole cells on the PDDA/glass interface by using MAPLE in certain experimental conditions, namely at intermediate fluences and for moderately long freezing time of bacterial suspensions. The layers deposited by MAPLE were less dense, having a different appearance than the ones deposited via LBL. Nonetheless, MAPLE-deposited bacteria preserved their sensitivity to lysozyme and led to similar results for the analysis of lysozyme in real serum samples as the reference interfaces modified via LBL. Compared to LBL, where the steps in slide functionalization were manually performed, MAPLE offers a good control of deposition. Given the importance of the sensing interfaces architecture MAPLE is promising for transferring in a controlled way other compounds to increase the stability and sensitivity of the interfaces for lysozyme detection in serum. The stabilizing role of the GO coating applied on ML-functionalized interfaces for sensing applications in serum was rationalized via Raman and optical microscopy analysis, showing that GO was anchored both on PDDA and on bacteria. Applications of MAPLE-deposited ML bacteria were illustrated through a 10-min assay where detection relies on the analysis of the sample spot intensity via an image analysis software. Future work will be centered on further simplifying the assay by using low cost plastic covers instead of glass slides and optimization of ML solution used as target in MAPLE, e.g. by including low concentration of DMSO (below 5%) to avoid cell breaking and ensure denser layers. This study paves the way for other whole cell biosensors and bioassays facilitated by MAPLE deposition.

Conflict of Interest

The authors declare that they have no conflict of interest.

Acknowledgments

Funding from the Romanian Ministry of National Education, CNCS – UEFISCDI, for the PN-II-PT-PCCA 239/2014, PN-II-PT-PCCA 213/2014 and TE 24/2014 projects and from the FlagEra for the “Graphtivity” project is gratefully acknowledged.

References

[1] E. Michelini, L. Cevenini, M.M. Calabretta, S. Spinozzi, C. Camborata, A. Roda, Field-deployable whole-cell bioluminescent biosensors: so near and yet so far, Anal Bioanal Chem, 405 (2013) 6155-6163.
[2] X. Liu, K.J. Germaine, D. Ryan, D.N. Dowling, Whole-cell fluorescent biosensors for bioavailability and biodegradation of polychlorinated biphenyls, Sensors (Basel), 10 (2010) 1377-1398.

[3] F. Lagarde, N. Jaffrezic-Renault, Cell-based electrochemical biosensors for water quality assessment, Analytical and Bioanalytical Chemistry, 400 (2011) 947.
[4] A. Qureshi, A. Pandey, R.S. Chouhan, Y. Gurbuz, J.H. Niazi, Whole-cell based label-free capacitive biosensor for rapid nanosize-dependent toxicity detection, Biosens Bioelectron, 67 (2015) 100-106.
[5] S. David, C. Polonschii, M. Gheorghiu, D. Bratu, A. Dobre, E. Gheorghiu, Assessment of pathogenic bacteria using periodic actuation, Lab on a Chip, 13 (2013) 3192-3198.
[6] L. Goers, C. Ainsworth, C.H. Goey, C. Kontoravdi, P.S. Freemont, K.M. Polizzi, Whole-cell Escherichia coli lactate biosensor for monitoring mammalian cell cultures during biopharmaceutical production, Biotechnol Bioeng, 114 (2017) 1290-1300.
[7] Q. Gui, T. Lawson, S. Shan, L. Yan, Y. Liu, The Application of Whole Cell-Based Biosensors for Use in Environmental Analysis and in Medical Diagnostics, Sensors (Basel), 17 (2017).
[8] S.K. Jha, M. Kanungo, A. Nath, S.F. D'Souza, Entrapment of live microbial cells in electropolymerized polyaniline and their use as urea biosensor, Biosens Bioelectron, 24 (2009) 2637-2642.
[9] S. Seuss, A.R. Boccaccini, Electrophoretic Deposition of Biological Macromolecules, Drugs, And Cells, Biomacromolecules, 14 (2013) 3355-3369.
[10] S. Saxena, Immobilisation and Biosensors, Applied Microbiology, Springer India, New Delhi, 2015, pp. 179-190.
[11] A. Khademhosseini, K.Y. Suh, J.M. Yang, G. Eng, J. Yeh, S. Levenberg, R. Langer, Layer-by-layer deposition of hyaluronic acid and poly-l-lysine for patterned cell co-cultures, Biomaterials, 25 (2004) 3583-3592.
[12] Y. Zhou, A. Marar, P. Kner, R.P. Ramasamy, Charge-Directed Immobilization of Bacteriophage on Nanostructured Electrode for Whole-Cell Electrochemical Biosensors, Analytical Chemistry, 89 (2017) 5734-5741.
[13] S. Szunerits, O. Zagorodko, V. Cogez, T. Dumych, T. Chalopin, D. Alvarez Dorta, A. Sivignon, N. Barnich, A. Harduin-Lepers, I. Larroulet, A. Yanguas Serrano, A. Siriwardena, A. Pesquera, A. Zurutuza, S.G. Gouin, R. Boukherroub, J. Bouckaert, Differentiation of Crohn's Disease-Associated Isolates from Other Pathogenic Escherichia coli by Fimbrial Adhesion under Shear Force, Biology, 5 (2016) 14.
[14] A. Avramescu, R. Rouillon, R. Carpentier, Potential for use of a cyanobacterium Synechocystis sp. immobilized in poly(vinylalcohol): Application to the detection of pollutants, Biotechnology Techniques, 13 (1999) 559-562.
[15] A. Piqué, The Matrix-Assisted Pulsed Laser Evaporation (MAPLE) process: origins and future directions, Applied Physics A, 105 (2011) 517-528.
[16] L. Rusen, P. Neacsu, A. Cimpean, I. Valentin, S. Brajnicov, L.N. Dumitrescu, J. Banita, V. Dinca, M. Dinescu, In vitro evaluation of poly(ethylene glycol)-block-poly(ε-caprolactone) methyl ether copolymer coating effects on cells adhesion and proliferation, Applied Surface Science, 374 (2016) 23-30.
[17] L. Rusen, V. Dinca, B. Mitu, C. Mustaciosu, M. Dinescu, Temperature responsive functional polymeric thin films obtained by matrix assisted pulsed laser evaporation for cells attachment–detachment study, Applied Surface Science, 302 (2014) 134-140.
[18] A.P. Caricato, R. Buonsanti, M. Catalano, M. Cesaria, P.D. Cozzoli, A. Luches, M.G. Manera, M. Martino, A. Taurino, R. Rella, Films of brookite TiO2 nanorods/nanoparticles deposited by matrix-assisted pulsed laser evaporation as NO2 gas-sensing layers, Applied Physics A, 104 (2011) 963-968.
[19] V. Dinca, P.E. Florian, L.E. Sima, L. Rusen, C. Constantinescu, R.W. Evans, M. Dinescu, A. Roseanu, MAPLE-based method to obtain biodegradable hybrid polymeric thin films with embedded antitumoral agents, Biomedical Microdevices, 16 (2014) 11-21.
[20] A. Palla-Papavlu, I. Paraico, J. Shaw-Stewart, V. Dinca, T. Savopol, E. Kovacs, T. Lippert, A. Wokaun, M. Dinescu, Liposome micropatterning based on laser-induced forward transfer, Applied Physics A, 102 (2011) 651-659.
[21] B. Hopp, T. Smausz, N. Kresz, N. Barna, Z. Bor, L. Kolozsvari, D.B. Chrisey, A. Szabo, A. Nogradi, Survival and proliferative ability of various living cell types after laser-induced forward transfer, Tissue Eng, 11 (2005) 1817-1823.
[22] A. Vasilescu, Q. Wang, M. Li, R. Boukherroub, S. Szunerits, Aptamer-Based Electrochemical Sensing of Lysozyme, Chemosensors, 4 (2016) 10.

[23] E. Kutter, Lysozyme A2 - Brenner, Sydney, in: J.H. Miller (Ed.) Encyclopedia of Genetics, Academic Press, New York, 2001, pp. 1131-1132.
[24] P. Mörsky, Turbidimetric determination of lysozyme with Micrococcus lysodeikticus cells: Reexamination of reaction conditions, Analytical Biochemistry, 128 (1983) 77-85.
[25] A. Vasilescu, S. Gáspár, M. Gheorghiu, S. David, V. Dinca, S. Peteu, Q. Wang, M. Li, R. Boukherroub, S. Szunerits, Surface Plasmon Resonance based sensing of lysozyme in serum on Micrococcus lysodeikticus-modified graphene oxide surfaces, Biosensors and Bioelectronics, 89 (2017) 525-531.
[26] G. Decher, Fuzzy Nanoassemblies: Toward Layered Polymeric Multicomposites, Science, 277 (1997) 1232-1237.
[27] O.S. Sakr, G. Borchard, Encapsulation of Enzymes in Layer-by-Layer (LbL) Structures: Latest Advances and Applications, Biomacromolecules, 14 (2013) 2117-2135.
[28] A.C. Ferrari, J. Robertson, Interpretation of Raman spectra of disordered and amorphous carbon, Physical Review B, 61 (2000) 14095-14107.
[29] G. Voortman, J. Gerrits, M. Altavilla, M. Henning, L. van Bergeijk, J. Hessels, Quantitative determination of faecal fatty acids and triglycerides by Fourier transform infrared analysis with a sodium chloride transmission flow cell, Clin Chem Lab Med, 40 (2002) 795-798.
[30] A. Barth, Infrared spectroscopy of proteins, Biochimica et Biophysica Acta (BBA) - Bioenergetics, 1767 (2007) 1073-1101.
[31] S. Garip, A.C. Gozen, F. Severcan, Use of Fourier transform infrared spectroscopy for rapid comparative analysis of Bacillus and Micrococcus isolates, Food Chemistry, 113 (2009) 1301-1307.
[32] M.A. Miguel Gómez, M.A. Bratos Pérez, Martı, x, F.J. n Gil, D. Dueñas, x, A. ez, Martı, x, R. n, x, J.F. guez, R. Gutiérrez, x, P. guez, A. Orduña Domingo, Rodrı, x, A. guez Torres, Identification of species of Brucella using Fourier transform infrared spectroscopy, Journal of Microbiological Methods, 55 (2003) 121-131.
[33] D.S. Liao, J. Raveendran, S. Golchi, A. Docoslis, Fast and sensitive detection of bacteria from a water droplet by means of electric field effects and micro-Raman spectroscopy, Sensing and Bio-Sensing Research, 6 (2015) 59-66.
[34] B. Porstmann, K. Jung, H. Schmechta, U. Evers, M. Pergande, T. Porstmann, H.-J. Kramm, H. Krause, Measurement of lysozyme in human body fluids: Comparison of various enzyme immunoassay techniques and their diagnostic application, Clinical Biochemistry, 22 (1989) 349-355.
[35] P. He, Y. Zhang, L. Liu, W. Qiao, S. Zhang, Ultrasensitive SERS Detection of Lysozyme by a Target-Triggering Multiple Cycle Amplification Strategy Based on a Gold Substrate, Chemistry – A European Journal, 19 (2013) 7452-7460.
[36] Q. Wang, P. Subramanian, A. Schechter, E. Teblum, R. Yemini, G.D. Nessim, A. Vasilescu, M. Li, R. Boukherroub, S. Szunerits, Vertically Aligned Nitrogen-Doped Carbon Nanotube Carpet Electrodes: Highly Sensitive Interfaces for the Analysis of Serum from Patients with Inflammatory Bowel Disease, ACS Applied Materials & Interfaces, 8 (2016) 9600-9609.
[37] Q. Wang, A. Vasilescu, Q. Wang, Y. Coffinier, M. Li, R. Boukherroub, S. Szunerits, Electrophoretic Approach for the Simultaneous Deposition and Functionalization of Reduced Graphene Oxide Nanosheets with Diazonium Compounds: Application for Lysozyme Sensing in Serum, ACS Applied Materials & Interfaces, 9 (2017) 12823-12831.
[38] E. Heydari-Bafrooei, S. Askari, Ultrasensitive aptasensing of lysozyme by exploiting the synergistic effect of gold nanoparticle-modified reduced graphene oxide and MWCNTs in a chitosan matrix, Microchimica Acta, 184 (2017) 3405-3413.